

Non-Newtonian phenomena in

Computer simulations indicate that simple liquids can display a surprising range of exotic nonequilibrium phenomena, more commonly seen in systems of macromolecules.

Denis J. Evans, Howard J. M. Hanley and Siegfried Hess

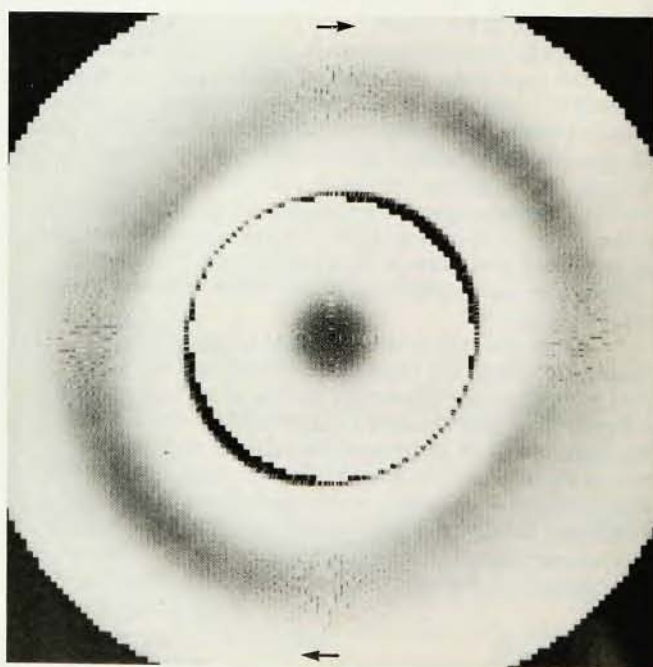
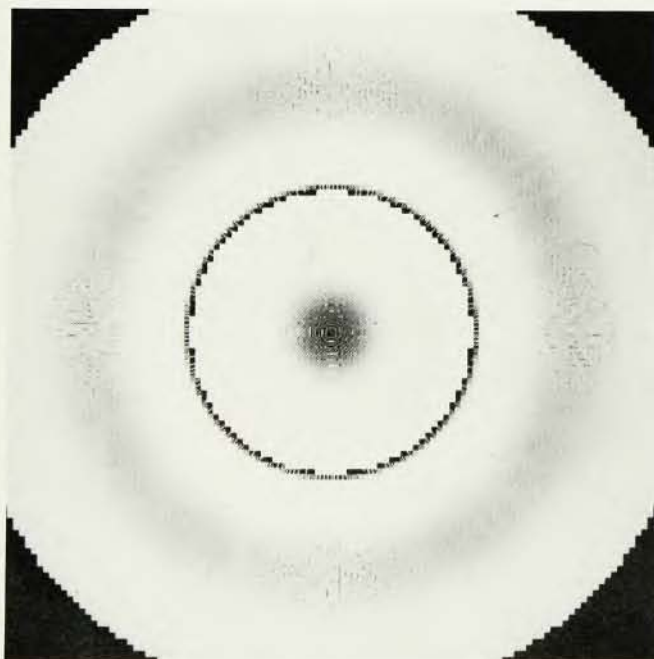
Almost a hundred years ago, Osborne Reynolds carried out a simple experiment.¹ He filled a leather bag with marbles, topped it with water and then twisted it, thereby inducing a shear. The water level drops because the close packing of the marbles is disrupted as layers of marbles slide over each other during the twisting motion; as a result the marbles are further apart on average, creating space that the water has to fill.

This experiment demonstrates the

Denis J. Evans is a fellow at the Research School of Chemistry, Australian National University, Canberra, Australia. Howard J. M. Hanley is a senior research chemist in the chemical engineering science division of the National Engineering Laboratory, National Bureau of Standards, Boulder, Colorado. Siegfried Hess is professor of theoretical physics at the Institut für Theoretische Physik der Universität Erlangen-Nürnberg, in Germany.

nonequilibrium non-Newtonian phenomenon known as shear dilatancy: The density (number of marbles divided by total volume, N/V) decreases when the system is subjected to a shear at constant pressure and temperature. We introduce it to bring up two points. The marble-water system models a dense hard-sphere liquid, so the first point is that the experiment illustrates that non-Newtonian behavior can be associated with simple fluids. The behavior arises from the distortion of the fluid structure, however, and is to be contrasted with intramolecular distortion often encountered in polymeric liquids—for example, a polymer unraveling under shear. The pioneers of fluid mechanics appreciated that the intermolecular structure of a fluid distorts under shear. James Clerk Maxwell, in particular, recognized that the mere existence of a shear viscosity

in an atomic fluid shows this. Second, the result of the experiment raises questions on the assumptions needed to describe a system out of equilibrium. For instance, it challenges the common postulate of local thermodynamic equilibrium. A complete study of the dynamics of the system must include the time-dependent behavior of thermodynamic variables (the internal energy and entropy in particular). The local equilibrium postulate is that these variables are defined with respect to position and time but are assumed to be related via the expressions of *equilibrium* thermodynamics and to obey the *equilibrium* equation of state. For the marble-water system, or for any dilatant fluid, the hydrostatic pressure is *not* the same function of state variables as it is at equilibrium. Equally, the thermodynamic potentials cannot be functions *solely* of the equilibrium ther-



simple fluids

modynamic state variables.

Other examples of simple systems that can be non-Newtonian are known. For instance, David Burnett showed fifty years ago that a dilute monatomic gas is shear thinning—that is, the viscosity decreases with strain rate—and exhibits normal stress effects—that is, the elements of the hydrostatic pressure are unequal. But the range of exotic nonequilibrium phenomena that a simple system can display has perhaps only become noticed as a consequence of computer simulations. (See

Density variation about a central particle for a fluid subjected to various amounts of shear. The darkness of the shading in these computer-generated plots indicates the relative probability of finding another particle at each point. In equilibrium (a) the distribution is radially symmetrical, with a maximum near 1.1 radii from the center. At low shear (b) the pattern is distorted (somewhat enhanced in the figure). The departure from a circle is a measure of the viscosity of the fluid. At high shear (c) the distortion becomes uneven and the maxima of the distribution pattern are displaced from the $\pi/4$ and $3\pi/4$ directions of case b. At high shear there is also a distortion of the correlation function in the y - z plane, perpendicular to the plane of the shear (d).

Figure 1

figure 1.) Simulations of model systems of spherical particles reveal a richness of behavior that mirrors qualitatively the fascinating rheological phenomena discussed by Byron Bird and C. F. Curtiss (page 36): shear dilatancy, shear thinning, normal pressure differences, visco-elasticity, and so on. In this article we describe some of the results. They are extracted largely from our own studies of a soft-sphere fluid and of a Lennard-Jones fluid, using the computer-simulation technique of nonequilibrium molecular dynamics. (See the article by W. G. Hoover, page 44.)

We studied the model fluids under shear by simulating what is called planar Couette flow: the flow between two infinite parallel plates with a linear fluid velocity profile of the sort shown in figure 2a. The strain rate tensor γ for the configuration has one non-zero element $\gamma_{xy} = \gamma = du_x/dy$ where u_x is the flow velocity in the x -direction.

A typical simulation evaluates the energy E and the pressure tensor \mathbf{P} for a system at constant density, temperature T and γ . The pressure tensor has two contributions: the isotropic (scalar) pressure p and the shear-stress tensor $\mathbf{\Pi}$. The pressure is defined as

one-third of the trace of the pressure tensor, and we can formally separate the contributions by writing

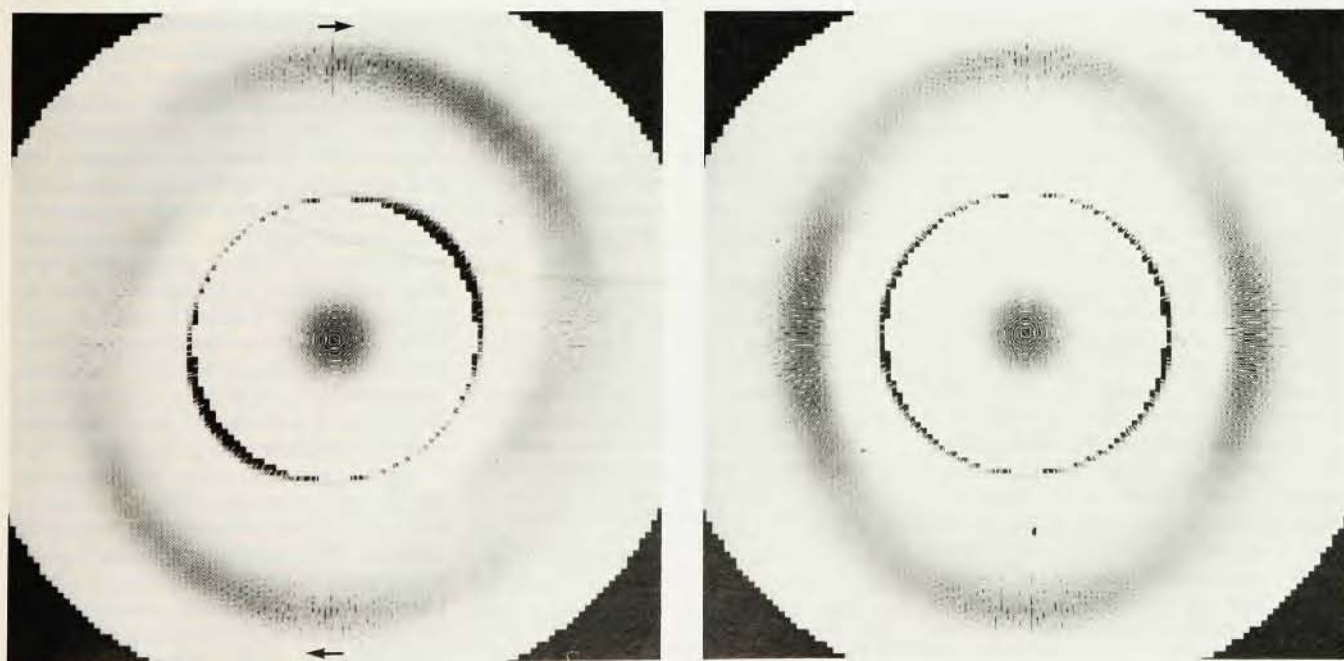
$$\mathbf{P} = p(\gamma)\mathbf{I} + \mathbf{\Pi}$$

\mathbf{I} is the unit tensor. The behavior of the shear viscosity coefficient, η , is of considerable interest and this coefficient is defined by the relation

$$\mathbf{\Pi} = -2\eta(\gamma)\gamma.$$

Note that the definitions of the pressure and viscosity allow for a dependence on the strain rate γ . One can also investigate the microstructure of the system by evaluating the pair correlation function or radial distribution function, g , and one can relate changes in microstructure, particularly on deformation, to the system's properties. One can also study other aspects of the flow with similar techniques. Time-dependent Couette flow, for example, can be investigated by setting the strain rate as some specified function of time.

We will not give computational details; they are described in Hoover's article (page 44). A feature, however, of our recent work is a reformulation of the laws of classical mechanics in which thermodynamic variables such as the temperature, the pressure and



the shear stress are constants of the motion. These variations turn out to be particularly useful in studying the thermodynamics of shear flows very far from equilibrium.

Fluid structure under shear

Let us consider first the microscopic structure of a fluid that can be subjected to a deformation due to an applied shear. The radial distribution function $g(\mathbf{r}_1, \mathbf{r}_2)$ represents the variation of the local microscopic density (that is, the structure) at a given macroscopic density and temperature. It gives the probability per unit volume that a particle is at position \mathbf{r}_2 if a particle is located at \mathbf{r}_1 . This probability is a function of the strain rate. For a homogeneous fluid, g depends only on the relative position of the two particles, that is on difference $\mathbf{r} = \mathbf{r}_2 - \mathbf{r}_1$ between their vector positions: hence $g = g(\mathbf{r}, \gamma)$. In equilibrium, when γ is zero, the radial distribution is solely a function of the distance $|\mathbf{r}|$ and not of direction. Figure 3 gives a typical schematic plot of $g(r)$ for a dense fluid of spherical particles at equilibrium. The plot for the marbles in Reynolds's experiment would be similar. Because the particles have a finite size, $g(r)$ is essentially zero for small r ; the peak in probability at distances just larger than the radius of the particle is due to its nearest neighbors; for larger radii the function oscillates, decaying to a constant value at large r . The function $g(r)$ is normalized such that a value of 1 means the local density is the macroscopic density. The decay in the distribution function indicates the short-range order in fluids and is the distinction between the structure of a fluid and that of a solid. For a dilute gas, on the other hand, $g(r) = 1$ for all values of r greater than the diameter of the particles, because a gas has no structure at all.

If the fluid is deformed it is essential to understand how $g(\mathbf{r}, \gamma)$ depends on the direction of \mathbf{r} . One approach is to expand $g(\mathbf{r}, \gamma)$ in terms of spherical harmonics, $y_{l,m}$, which separate the scalar (nondirectional) and tensor (directional) contributions. If the particles are indistinguishable their distribution must be symmetrical, and only terms of even l occur in the expansion. The lowest-order term ($l=0$) is the scalar contribution; its value $g^{(s)}$ is the average of $g(\mathbf{r}, \gamma)$ over all directions. For the next order, the terms for $l=2$, there are in general five coefficients, but only three contribute in planar Couette flow. These are associated with the directional dependences of the form $r_x r_x / r^2$, $(r_x^2 - r_y^2) / r^2$ and $r_z^2 / r^2 - 1/3$. The coefficients are denoted by g_+ , g_- and g_0 , respectively.

One can link the coefficients with the macroscopic properties of the fluid.

These properties depend on the intermolecular forces—or the intermolecular potential function $\phi(\mathbf{r})$ —weighted by the number of particles to be found at any distance \mathbf{r} from a chosen particle: the radial distribution function. Two examples: the pressure is

$$p \sim \int \phi' g^{(s)} r^3 dr$$

and the shear viscosity is

$$\eta \sim \int \phi' g_+ r^3 dr$$

To clarify the physical picture of deformation in a fluid it helps to digress slightly and remark on Maxwell's ideas:

According to Poisson's theory of internal friction in fluids, a viscous fluid behaves as an elastic solid would do if it were periodically liquefied for an instant and solidified again, so that at each fresh start it becomes for the moment like an elastic solid free from strain.

In our notation, we would say that the structure of the fluid under a strain rate γ is identical to the structure of a glass under a strain $\tau\gamma$, where τ is a phenomenological relaxation time. For example, consider a fluid at rest characterized by an equilibrium distribution function $g_e(r)$. Suppose a parti-

cle originally at \mathbf{r}' is shifted on deformation so that $\mathbf{r}' \rightarrow \mathbf{r}$. The hypothesis is that $\mathbf{r}' = \mathbf{r} - \tau\gamma\mathbf{r}$. We thus expect the correlation function to be

$$g(\mathbf{r}, \gamma) = g_e(\mathbf{r} - \tau\gamma\mathbf{r})$$

and expanding to linear order

$$g(\mathbf{r}, \gamma) = g_e(r) - \tau\mathbf{r} \cdot \gamma (dg_e/dr)$$

The term g_e is equivalent to the coefficient $g^{(s)}$ from a spherical harmonic expansion; the term $-\gamma r (dg_e/dr)$ is equivalent to the shear-viscosity expansion coefficient g_+ . As one might expect, and as we will show, the Maxwell hypothesis is too simple, but the results from computer simulations indicate it gives a very reasonable picture of a distorted fluid under low strain rates, and represents the coefficient g_+ remarkably well even for high strain rates.

Microstructure. Figure 1 shows what happens to $g(\mathbf{r}, \gamma)$ when a model soft-sphere fluid close to its freezing density is sheared. The soft-sphere fluid has an intermolecular potential ϕ that behaves as $1/r^n$ where $n=12$ in our simulations. It is important to stress that the actual choice of the model fluid is not too significant in this context: It is well known that the form of the radial distribution function is only weakly dependent on details of the potential function.

Figure 1a shows the structure for $\gamma = 0$; that is, it depicts the equilibrium radial distribution function for the fluid at rest. The darkness in a region is a measure of the chances of finding a particle in a given volume with respect to the average number of particles per unit volume: the darker the shading, the greater the probability. The center spot represents a reference central particle. The graph is radially symmetric as one would expect. The first coordination shell, given by the peak in g for r near 1.1 in figure 3, is clearly seen as the darkest area.

Let us now apply a shear to the fluid. Figure 1b represents structure for a sheared fluid in the plane of the shear, the x - y plane, in the linear region close to equilibrium. The intensity pattern is elliptical and reveals an increased probability of finding particles in the first and third quadrants. This is consistent with Maxwell's idea for the deformation of the equilibrium distribution; the principal axes of the elastic deformation are, as predicted by Maxwell, at $\pi/4$ and $3\pi/4$. The distortion away from the circle is related to the shear viscosity and to the product of the strain rate γ and the relaxation time τ , which is a measure for the lifetime of such an elliptical distortion of the pair-correlation function. This relaxation time could, in principle, be obtained by measuring how $g(\mathbf{r}, \gamma)$ of figure 1b relaxes back to $g(r)$ of figure 1a after a

Asymptotic behavior

We present here some results from non-equilibrium molecular dynamics for the asymptotic behavior of some properties of a d -dimensional liquid undergoing planar Couette flow. (The absolute value of the strain rate is γ .)

$$d = 2$$

$$\begin{aligned}\eta(\gamma) &= -A \log(B\gamma) \\ p(\gamma) &= p(0) + A\gamma \log(B\gamma) \\ E(\gamma) &= E(0) + A\gamma \log(B\gamma)\end{aligned}$$

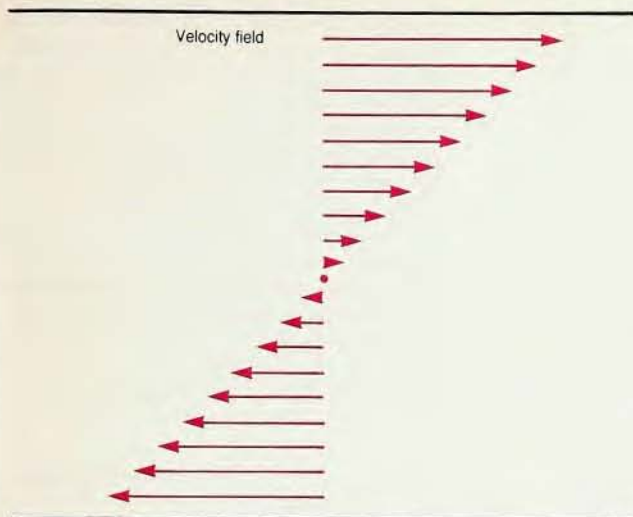
$$d = 3$$

$$\begin{aligned}\eta(\gamma) &= \eta(0) - A\gamma^{1/2} \\ p(\gamma) &= p(0) + A\gamma^{3/2} \\ E(\gamma) &= E(0) + A\gamma^{3/2} \\ \hat{\eta}(\omega) &= \eta(0) - A(\omega)^{1/2} \\ \eta(k) &= \eta(0) - Ak^{3/2}\end{aligned}$$

$$d = 4$$

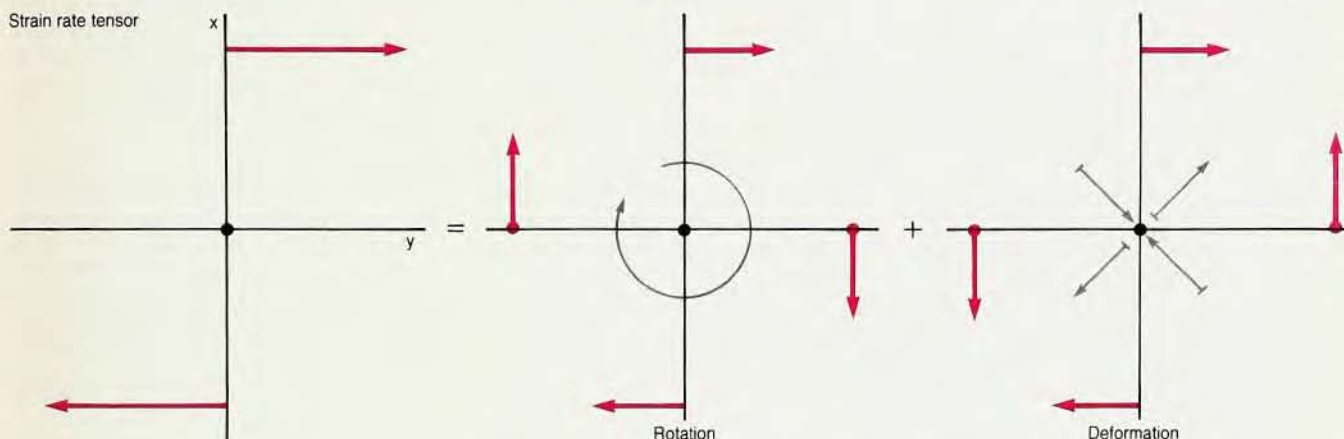
$$\begin{aligned}\eta(\gamma) &= \eta(0) - A\gamma \\ p(\gamma) &= p(0) + A\gamma \\ E(\gamma) &= E(0) + A\gamma\end{aligned}$$

All these results pertain to the limiting behavior as γ , ω and k become vanishingly small. Thermodynamic instabilities restrict the range of γ over which these processes can be observed. We have used A and B simply to refer to positive constants unique to each equation. We have included the behavior of the viscosity as a function of wavevector. We include it in the table as a matter of interest, although we have not discussed in the article.



Couette flow is the motion of a fluid between two infinite parallel plates moving in opposite directions. We show the resulting velocity field and the decomposition of the strain-rate tensor into a "rotation" and "deformation." The strain-rate tensor is the gradient of the velocity; here it has only one non-zero component, $\gamma = du_x/dy$; the "rotation" and "deformation" are the antisymmetric and symmetric traceless parts of the tensor.

Figure 2



sudden removal of the strain.

We could also have shown plots for cross sections perpendicular to the plane of the shear. However, we have verified—again for small shear—that they are circular patterns identical to that shown in figure 1a, again consistent with the Maxwell hypothesis.

At high shear rates, one obtains patterns such as those of figures 1c and 1d, for the x - y and y - z planes respectively. Compare figure 1c with figure 1b. The deformation of $g(\mathbf{r}, \gamma)$ is greater, and the principal axes of the deformation are changed. Figure 1d shows that even perpendicular to the shear plane the shear rate is large enough to introduce distortion. Both of these features indicate a breakdown of the simple Maxwell picture and indicate that the coefficients g_- and g_0 , which appear in the spherical-harmonic expansion for $l=2$, cannot be zero. It is precisely the appearance of these terms that signals the presence of non-Newtonian phenomena.

It is not surprising that the simple Maxwell analogy eventually fails. Despite the apparent similarity of our results with what one would expect for a solid (glass) under shear, there is an important difference that should be stressed here: For a fluid undergoing a

stationary viscous flow, $g(\mathbf{r}, \gamma)$ represents a static picture of an underlying dynamic phenomenon.

A qualitative understanding² of the origins of these non-Newtonian distortions can be obtained by realizing that the strain-rate tensor has an antisymmetric part associated with the vorticity ω , defined as $\frac{1}{2}\nabla \times \mathbf{u}$, and a symmetric (traceless) part, which is the (scalar) strain rate. For a pictorial representation of this decomposition in planar Couette flow see figure 2. The physical effects associated with the two contributions (which both are proportional to γ) are quite distinct: the vorticity induces a rotation, the shear-rate tensor a deformation. In the regime in which the flow is linear, only the deformation is "felt" by the fluid and this causes the elliptical distortion of $g(\mathbf{r})$ described above. In the case of nonlinear flow, the vorticity ω causes a rotation of the primarily distorted structure away from the $\pi/4$ and $3\pi/4$ directions; this generates the g_- term of a spherical-harmonic expansion. Further deformation of the already deformed structure generates the g_0 term.

Irreversible thermodynamics

A long-standing goal has been to set

up a macroscopic nonequilibrium theory in the spirit of thermodynamics, not only for its own sake but to put transport and nonequilibrium behavior, such as the distortion of fluid microstructure, in a consistent perspective. Until recently, however, the only practical theory of irreversible thermodynamics rested on the assumption that local equilibrium holds and that the state variables of a system out of equilibrium have the same functional relationships as they have when the system is in equilibrium. However, these assumptions can only be approximations and do not hold either in the Reynolds experiment or in the computer simulations at high shear. In fact, we know how to compute the difference in the thermodynamic mechanical properties, such as the hydrostatic pressure and the energy, from their equilibrium values if we know the dependence of the radial distribution on the strain rate. This difference is very real and significant.

However, a practical, *verifiable* heuristic thermodynamics has been proposed.³ It is based on the following:
► We observed from the molecular-dynamics simulations that the energy is a state function of the strain rate; in particular $E = E(V, T, \gamma)$

- We know that thermodynamic potentials are scalar quantities, even for a shearing fluid far from equilibrium
- We also know that a fluid undergoing a shear cannot distinguish thermodynamically between the work done by compressions acting along different directions relative to the shear
- The Poisson–Maxwell concept assumes a fluid under shear has a structure similar to a pseudo-equilibrium fluid that has been subjected to a strain; we therefore expect a thermodynamics of a sheared fluid to be at least qualitatively similar to that of a strained material; the latter is standard.⁴

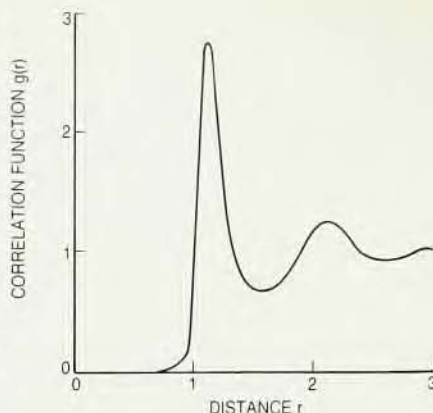
In short, we postulated that the first and second laws of thermodynamics should be modified for fluids to become

$$dE = dQ - pdV + \zeta d\gamma \quad (1)$$

where dQ is the total heat adsorbed by the fluid; the pressure is defined formally as one-third of the trace of the pressure tensor. Further, we postulate an entropy S by $TdS > dQ$.

We propose equation 1 only for steady states. Thus, for example, if we achieved the steady state by subjecting the system to a constant strain rate at a constant density and keep the temperature constant by means of a thermostat, dQ must be zero, and the heat produced in the system by the shear must be removed exactly by the thermostat.

The quantity ζ is a strain-rate “potential” defined formally as the derivative of the energy E with respect to the strain rate, at constant entropy and volume. It is a quantitative measure of the cost in free energy required to pass between steady states that differ in the strain rate; this cost in turn is a reflection of the rearrangements in the fluid structure as the strain rate is changed. In more detail, suppose the system changes from one steady state (N, V, T, γ_1) to another (N, V, T, γ_2) . We imagine this change occurs through an infinite sequence of intermediate quasisteady states (N, V, T, γ_i) . In the i th intermediate state, once the state has been established the net heat gained or lost by the system must once again vanish, and there must be exact balance between the viscous heat produced by the shear and the heat removed by the thermostat. However, we know from the earlier discussion that at constant density, volume and temperature, the radial distribution function $g(r; N, V, T, \gamma)$ changes as the system passes from state $i-1$ to state i . Further, we know that changes in $g(r)$ will necessarily be associated with changes in the internal energy and pressure. Evidently the balance between the internally generated heat from viscosity and the heat removed by the thermostat is upset during the



Equilibrium radial distribution function $g(r)$: given a particle at $r=0$, what is the relative probability that a second particle is at the distance r from the first? In a dense fluid, the best chance is at 1.1 radii away from the center. (The distance units are normalized to the diameter of the particles.) Figure 3

establishment of the new state i from $i-1$ (otherwise energy conservation would be violated). Some of the viscous heat apparently provides the energy required for the structural rearrangement of the new steady state. Thus the system absorbs net heat during the quasisteady change $1 \rightarrow \dots \rightarrow 2$.

Unfortunately it is very difficult to construct this type of experiment and

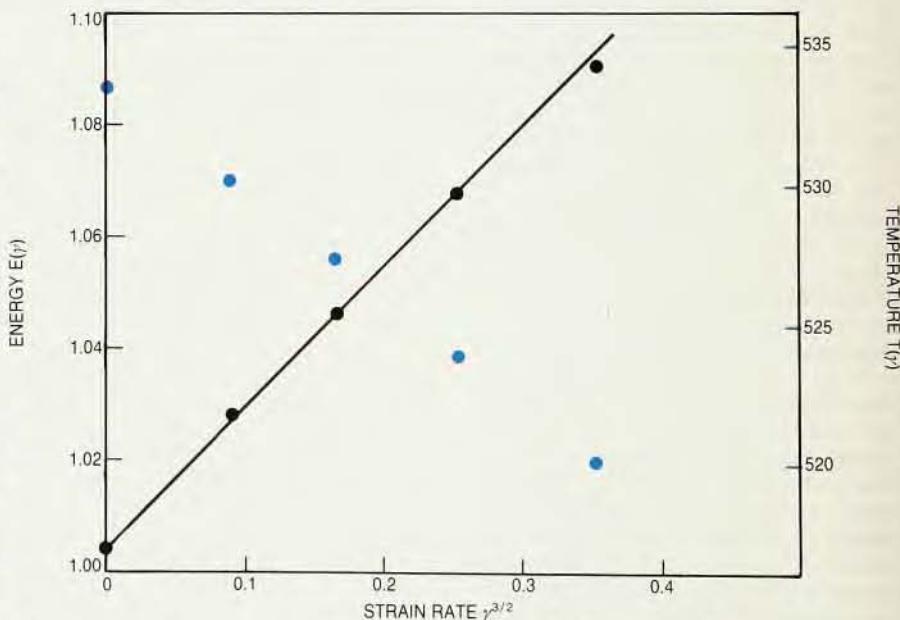
to evaluate free-energy differences directly. It is simpler to apply the usual thermodynamic analysis and, from a knowledge of various interrelationships of thermodynamic variables, calculate the required properties. For instance, the strain-rate potential follows from the Helmholtz free energy, and one can use the fact that the pressure is determined solely by the temperature and density in the dilute gas limit to evaluate it. In this way one can show that

$$\zeta(T, V, \gamma) = \int_V \frac{\partial p}{\partial \gamma} (V', T, \gamma) dV' + C(T, \gamma) \quad (2)$$

The term $C(T, \gamma)$ represents the ideal-gas component of ζ .

There are several consequences of equation 1; in particular, one can derive from it thermodynamic interrelationships and consistency checks, which can be tested numerically via computer simulation. Here we will mention three.

► The strain-rate potential ζ must be positive. The computer simulations appear to confirm this. Semiquantitative calculations of ζ have been made for simple model fluids, such as the soft-sphere and Lennard–Jones liquids. We will not show the results here but it appears that ζ is indeed positive and is a strong function of density at high densities and a relatively weak function of temperature.



Energy as a function of shear. The black dots are the result of molecular-dynamics calculations of the energy of a Lennard–Jones fluid at its triple point at constant temperature and volume (left-hand scale); the energy increases as $\gamma^{3/2}$. The blue spots are results of a calculation of temperature at constant energy and volume (right-hand scale). As equation 3 predicts (see text), the temperature decreases with increasing strain. The straight line is a prediction of the energy from an independent calculation of the specific heat, again using equation 3 to compute E from $C_{V\gamma}$. The fit is clearly excellent. (The units for these computer-generated graphs are normalized to standard values.) Figure 4

► The following relation should hold

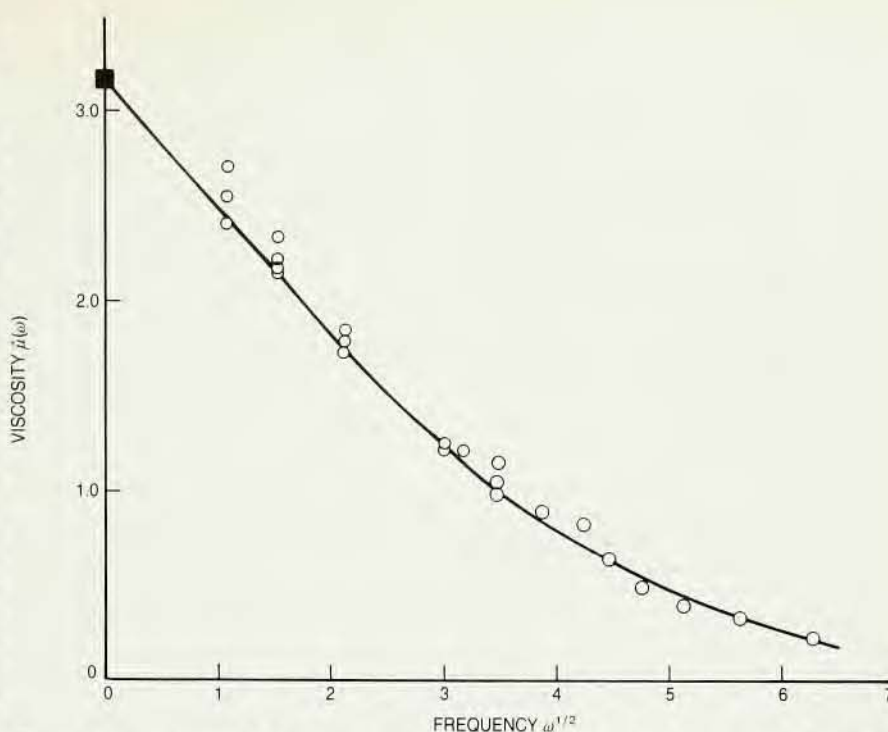
$$\left(\frac{\partial T}{\partial \gamma}\right)_{E,V} = -\left(\frac{\partial E}{\partial \gamma}\right)_{T,V} \left(\frac{1}{C_{v,\gamma}}\right) \quad (3)$$

where $C_{v,\gamma}$ is the specific heat at constant volume and shear rate. The equation leads to the perhaps surprising prediction that if the energy *increases* with shear at constant temperature and density, the temperature should *drop* with increasing shear rate at constant temperature, volume and internal energy. A test of equation 3 is represented by figure 4 which shows the direct molecular-dynamics calculation (shown as black dots) of the energy as a function of the strain rate at constant temperature and volume for the soft-sphere liquid close to its freezing. The energy increases with strain rate according to $\gamma^{3/2}$. The red dots in the figure are the direct calculations of the temperature as a function of strain rate at constant energy and volume. One sees that the temperature also varies as $\gamma^{3/2}$ and does in fact decrease, in agreement with the thermodynamics. Furthermore, using a separate calculation of $C_{v,\gamma}(\gamma)$ and the results for the variation of $T(\gamma)$, we predicted $E(\gamma)$ from equation 3. The prediction is shown as the curve in the figure. The thermodynamic prediction is in excellent agreement with the direct simulation.

► From a study of thermodynamic fluctuations about a steady state for a fluid undergoing Couette flow, we have concluded that if the pressure varies with the strain rate as γ^m at constant temperature and density, then m is strictly less than two. All the results from simulation, for many model fluids, are consistent with this conclusion. For a three-dimensional dense liquid, the pressure seems to vary as $\gamma^{3/2}$, consistent with the energy variation shown in figure 4. The variation of the pressure is thus nonanalytic.

Viscosity coefficients

The prophet Deborah remarked that the mountains flow before the Lord. Not only did she realize a similarity between the solid and the liquid via the concept of a time dependence, she also appreciated the idea of a time scale: the mountains flow, but on the Lord's time scale, not man's.⁵ The Deborah number for a material is the ratio between a characteristic time for a process and an observation time. If the characteristic time is taken⁶ as the time particles remain in a given equilibrium configuration before moving by diffusion to another, and if the observation time is, as it usually is, of the order of seconds, then a large Deborah number is associated with solids and a small number with liquids. But clearly, we can make the observation time very short, effectively increasing the De-



Frequency dependence of the viscosity of the Lennard-Jones fluid at its triple point. At low frequencies the viscosity appears to vary as the square root of the frequency. (The units for these computer-generated graphs are normalized to standard values.) Figure 5

borah number. Consequently, as was appreciated long ago, a fluid can respond elastically, like a solid, when a mechanical force is suddenly applied. Over a longer time the fluid cannot support the force and will flow. A fluid is thus viscoelastic. The phenomenon is often illustrated⁷ in textbooks by a simple model called a "Maxwell element." The model consists of a spring connected in series to a dashpot (a piston in a cylinder). Stretching the spring represents elastic deformation, moving the piston represents viscous flow. Note that stretching a spring can be considered a time-independent and essentially reversible effect, whereas moving the piston is time dependent and irreversible. If one stretches the element suddenly, only the spring can respond, and the model behaves like a solid. If the extension rate is small, however, the spring does not extend appreciably, but the piston moves—that is, the model represents the liquid. We can write for the dashpot $\Pi = -\eta\dot{\gamma}$ and for the spring $\Pi = -G\epsilon$ where G is the shear modulus and ϵ is the strain. Because the rate of change of ϵ is just $\dot{\gamma}$, the two relations can be combined and solved. The solution gives the relaxation time τ as η/G . To a first approximation this is the characteristic time of a material and is also the time a distorted fluid microstructure takes to relax to its equilibrium configuration.

As with other analogies of the fluid with a solid one should be cautious in carrying the analogy too far. It does exclude the dynamic nature of a fluid's

response to a shear, and it excludes the concept of a fluid element rotating under deformation.

The most general (but linear) relationship between stress and strain rate is⁸

$$\Pi(t) = - \int_0^t \eta(t-s)\dot{\gamma}(s)ds \quad (4)$$

The time-dependent kernel is called the viscosity memory function. This constitutive relation shows that the stress $-\Pi(t)$ is not only proportional to the concurrent value of the strain rate $\dot{\gamma}(t)$ but rather is a linear functional of the strain-rate history.

This memory function can be written more compactly by performing a Fourier transform to the frequency domain:

$$\Pi_{xy}(\omega) = -\hat{\eta}(\omega)\hat{\gamma}(\omega) \quad (5)$$

The time-independent Newtonian viscosity is just the zero-frequency limit of $\hat{\eta}(\omega)$.

In the linear regime, the memory function is given by the so called Green-Kubo relations which involve the equilibrium stress autocorrelation, that is, by expressions of the form

$$\langle \Pi(t+t')\Pi(t) \rangle$$

The Green-Kubo relations immediately tell us that *all* fluids are viscoelastic because equilibrium stress fluctuations must take a finite time to decay. The reciprocal of this decay time gives the characteristic frequency for the changeover from viscous to elastic response in a fluid. Maxwell was the first to realize that memory is the origin of viscoelasticity and that the real and

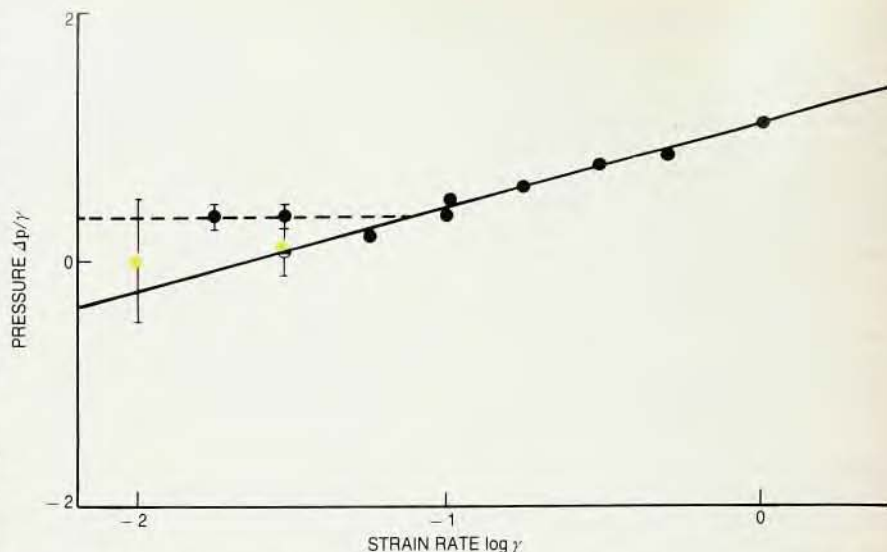
imaginary parts of $\hat{\eta}(\omega)$ describe respectively the viscous and elastic response of the fluid.

The Green-Kubo expressions are powerful and E. G. D. Cohen (page 64) and Berni J. Alder (page 56) discuss some of their consequences. The expressions only pertain to the limiting, linear regime close to equilibrium, however, and corresponding fluctuation relations for nonlinear transport coefficients are not known. Consequently the only method for calculating nonlinear transport coefficients known at present is nonequilibrium molecular dynamics.

To illustrate the variation of $\hat{\eta}$ over a wide range of ω , we show in figure 5 $\hat{\eta}(\omega)$ as calculated by molecular dynamics for the Lennard-Jones fluid at its triple point. The viscosity appears to vary as the square root of the frequency at low frequencies. From equations 4 and 5 we see that behavior as $\omega^{1/2}$ at low frequencies implies a slow, algebraic decay as $t^{-3/2}$ of the memory function $\eta(t)$, at long times.

Actually, slow, $t^{-3/2}$ decays of memory functions were first observed in equilibrium calculations of the memory function for self-diffusion by Alder and Thomas E. Wainwright. This "long-time tail" is thought to be common to the memory function of all Navier-Stokes transport coefficients. Theorists currently believe that highly collective (hydrodynamic) processes are responsible for these long-time tails. The exponent governing the decay appears to be independent of the nature of the interaction potential—depending instead upon more general quantities such as the dimensionality of the system.

For comparison, figure 6 gives the variation of the viscosity $\eta(\gamma)$ as a



Pressure of a two-dimensional soft-disc liquid as a function of strain rate. The liquid is near its freezing point. At high strain rate $\Delta p = p(\gamma) - p(0)$ varies as $\gamma \log \gamma$, but at low strain rates $\Delta p/\gamma$ is essentially independent of γ . The authors believe the change represents a thermodynamic instability consistent with the formalism described in the text. The colored dots indicate another extrapolation to low γ , an extrapolation for which the instability has been suppressed. (The units for these computer-generated graphs are normalized to standard values.) Figure 7

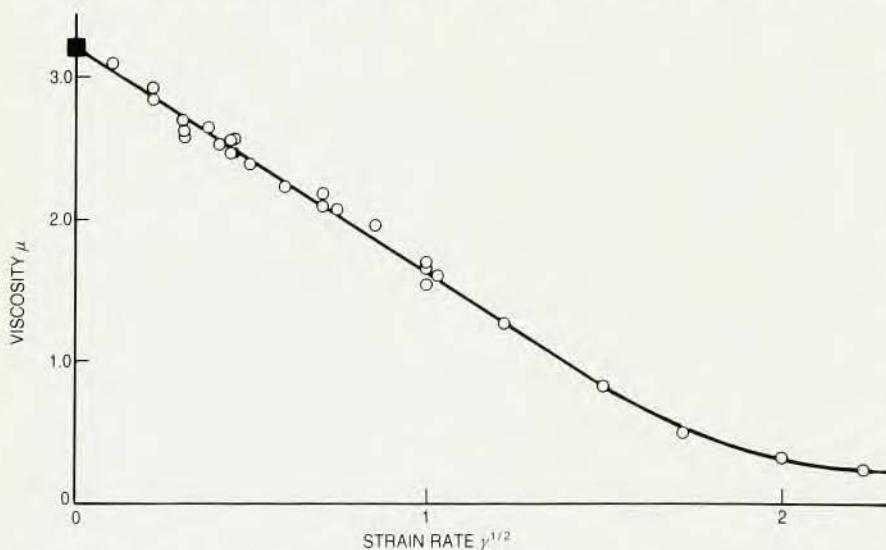
function of the strain rate, again for the Lennard-Jones fluid at the triple point. Nonanalytic behavior is seen once more, with the viscosity varying as the square root of the strain rate. In rheological terms, the Lennard-Jones fluid is "shear thinning." What is perhaps surprising is that the viscosity appears to vary as the square root of the strain rate until it is only 10 percent of its limiting zero shear rate value. This result implies that the Burnett expansion of $\eta(\gamma)$ (a Taylor series expansion of η in powers of γ) is divergent. There is an interesting debate on the possible relationship

between the coefficients for the $\omega^{1/2}$ term of $\hat{\eta}(\omega)$ and the $\gamma^{1/2}$ term for $\eta(\gamma)$. We should mention that, while current theory predicts correctly the exponents in figures 4–6, there is as yet no theory which predicts correctly the amplitude of the tails implied in the figures.

Two and four dimensions

Finally, let us note that one of the fascinating aspects of computer simulation is the possibility of obtaining "experimental data" for systems that do not occur in nature yet are amenable to theoretical analysis. One can get results which, although artificial, can lead to a better insight to the phenomena concerned. The work we have described here lends itself to such a treatment. We have seen that the properties of a sheared system depend on the applied force through appropriate exponents, which, however, apparently depend on the dimensionality of the system rather than on the nature of the fluid. We thus conclude our discussion with some results for the two-dimensional soft disc fluid and for the four-dimensional fluid. We will show the results are consistent with the thermodynamic consequences of the previous section.

Figure 7 shows the pressure for a system of soft discs close to the freezing transition undergoing Couette flow. The graph indicates that at high strain rates $p(\gamma)$ varies as $\gamma \log \gamma$. Below a critical strain rate, close to where the pressure would become less than the corresponding equilibrium pressure, the pressure becomes essentially independent of strain rate. However, this



Strain-rate dependence of the viscosity of the Lennard-Jones fluid at its triple point, and at zero frequency. (The intercept here is the same as in figure 5.) The viscosity varies as the square root of the strain rate over a wide range. (The units for these computer-generated graphs are normalized to standard values.) Figure 6

phenomenon is to be expected! The thermodynamics predicts that the strain-rate potential ξ is positive. If $p(\gamma)$ goes as $\gamma \log \gamma$, then equation 2 predicts thermodynamic instability for small enough strain rates. So the $\gamma \log \gamma$ dependence cannot hold for low values of γ . Furthermore, we believe that the instability at low γ manifests itself by the flow's developing convective cells, so that it is no longer planar Couette flow below the critical strain rate. Moreover, we can sense the onset of these convective cells in a further computer simulation by using Maxwell demons. We set up these demons to exert transverse forces that restore the planarity of the flow. When we perform the simulation under these conditions, we see the logarithmic functional forms over the entire range of strain rates.

As an aside, we remark that this thermodynamic instability is peculiar to two dimensions and is qualitatively different from the onset of Reynolds turbulence in three-dimensional systems at high shear rates. The thermodynamic instability occurs at low shear rates in a finite range of shear rates about the equilibrium state. Its onset is related to thermodynamic properties intrinsic to the fluid and the dimensionality of the system, not to a macroscopic length scale as in Reynolds turbulence.

A summary of all the constitutive relations observed by us is given in the box on page 28. We find that four dimensions $\eta(\gamma)$ and $p(\gamma)$ vary linearly as γ . Again we find that the dilatancy exponent is less than two, in agreement with the thermodynamic inequality.

* * *

Part of this work was carried out at the National Bureau of Standards and was supported by the Department of Energy, Office of Basic Energy Sciences. The Office of Standard Reference Data (National Bureau of Standards) sponsored segments of the program in its early stages. We are grateful to Karen Bowie and Dave Obitts for their help in preparing the article.

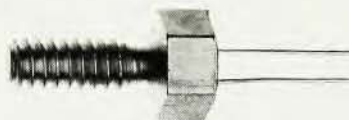
References

1. O. Reynolds, *Phil. Mag.* **20**, 469 (1885).
2. S. Hess, *Physica* **118A**, 79 (1983).
3. H. J. M. Hanley, D. J. Evans, *J. Chem. Phys.* **76**, 3225 (1982); D. J. Evans, *J. Chem. Phys.* **78**, 3297 (1983).
4. See, for example, J. Kestin, *A Course in Thermodynamics*, Blaisdell, Waltham, Mass. (1966), chapter 8.
5. C. A. Truesdell, *Rheology Volume 1*, Asarita, G. Marrucci, L. Nicolais, eds., Plenum, New York, (1980) page 1.
6. J. Frenkel, *Kinetic Theory of Liquids*, Dover, New York, (1955) chapter 4.
7. G. Harrison, *The Dynamic Properties of Supercooled Liquids*, Academic, London, (1976).
8. R. Zwanzig, R. D. Mountain, *J. Chem. Phys.* **43**, 4464 (1965). □

CRYOGENIC TEMPERATURE SENSORS

to meet your needs.

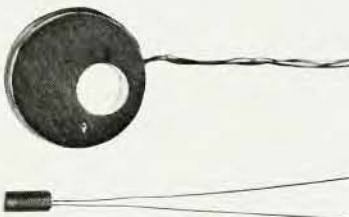
Silicon Diodes. Wide 1.4K to 380K range with sensitivity to 50mV/K below 30K. Available calibrated, uncalibrated, or matched to standard curves. Over 14 configurations.



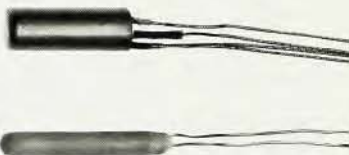
Germanium. Repeatability better than 0.5mK. LHe resistances from 50 to 2500 ohms. Available calibrated or uncalibrated in two sizes.



Carbon Glass. Monotonic over 1K to 300K range. Extremely low and predictable magnetic field dependence. Eight values allow temperature response to be optimized for a given use range.



Complete Line. Gallium-Arsenide Diodes, Platinum and Rhodium-Iron RTD's, Capacitance Sensors, plus a completely-equipped standards lab for calibrations from 0.05K to 380K. Sensors shown are enlarged to 1.5X to show detail.



The reliability of Lake Shore's cryogenic temperature sensors is the foundation of our reputation. Careful research into design, construction, and use assures predictable performance users can count on. So when you need sensors that make sense, come to Lake Shore . . . we know cryogenics COLD!

Cryogenic Thermometry • Instrumentation • Calibrations

 Lake Shore
Cryotronics, Inc.

64 E. Walnut St., Westerville, OH 43081 • (614) 891-2243

In Europe: Cryophysics: Witney, England • Jouy en Josas, France
Darmstadt, W. Germany • Geneva, Switzerland

In Japan: Niki Glass Co., Shiba Tokyo

Circle number 18 on Reader Service Card